

Biosyngas Utilization in Solid Oxide Fuel Cells with Ni/GDC Anodes

J.P. Ouweltjes, P.V. Aravind, N. Woudstra, G. Rietveld

Published in Journal of Fuel Cell Science and Technology, 3, (2006), 495-498

Februari 2007

Biosyngas Utilization in Solid Oxide Fuel Cells with Ni/GDC Anodes

JP Ouweltjes, PV Aravind*, N Woudstra* and G Rietveld

Energy Research Centre of the Netherlands ECN
P.O. Box 1, 1755 ZG Petten, The Netherlands

* Delft University of Technology, Energy Technology Section
Mekelweg 2, 2628 CD Delft, The Netherlands

telephone: (+31) 224 564064, fax (+31) 224 564965, email: ouweltjes@ecn.nl

The combination of biomass gasification systems with fuel cells promises adequate systems for sustainable, decentralized energy conversion. Especially high temperature fuel cells are suited for this task because of their higher tolerance to impurities, their internal steam reforming potential, and favorable thermal integration possibilities. This paper presents the results of biosyngas utilization in solid oxide fuel cells with Ni/GDC anodes at 850 and 920°C. The relation between the fuel composition and the electrochemical performance is discussed, as well as the impact of sulfur up to a concentration of 9 ppm H₂S. The investigations have made clear that Ni/GDC anodes can be operated within a wide range of biosyngas compositions. Sulfur has appeared to deactivate the anode for methane reforming. The oxidation of hydrogen and carbon monoxide are insensitive to sulfur, suggesting that both nickel and GDC are active electrocatalysts.

Keywords: SOFC, Biomass Gasifier, Biosyngas, Producer Gas, Sulfur Poisoning

Introduction

Economical conversion of biomass and agricultural residues requires either cheap decentralized combined heat and power plants or highly efficient centralized power plants. The combination of biomass gasification systems with high temperature fuel cells like the solid oxide fuel cell (SOFC) are an attractive option, as they provide better options for thermal integration [1], allow for carbon monoxide in the fuel gas stream and are capable of internal methane reforming [2,3]. It is still unknown to what extent the gas has to be cleaned on trace compounds like dust, sulfur, alkalis, halides and higher hydrocarbons. This paper describes the use of biosyngas, or producer gas, in planar SOFC membranes with Ni/GDC anodes. First, the anode catalytic and electrochemical activity for the conversion of the main components in biosyngas are discussed, as well as the impact of sulfur. Second, the performance under two synthetic biosyngas compositions are evaluated.

Experiments

The tests were performed with circular shaped, electrolyte supported cells with screen printed electrodes from InDEC, with a diameter of 120 mm and an active area of 100 cm². The electrolyte was 90 µm thick Y_{0.06}Zr_{0.94}O₂ (3YSZ) with at least 97 vol% density. The cathode was 40 µm thick and consisted of two layers. The cathode functional layer consisted of La_{0.75}Sr_{0.2}MnO₃ (LSM) and Y_{0.16}Zr_{0.84}O₂ (8YSZ) composite. The cathode current collecting layer consisted of LSM alone. The anode was also 40 µm thick and consisted of three layers. The functional layer consisted of nickel and Gd_{0.1}Ce_{0.9}O₂ (10GDC). Between the functional layer and the electrolyte, a layer consisting of Gd_{0.4}Ce_{0.6}O₂ was put to improve anode adherence. On top of the functional layer a pure nickel layer was applied to improve electrical contact. Figure 1 shows micrographs of both electrodes.

The membranes were tested in a ceramic cell housing, with alumina flanges for gas distribution, platinum gauze for cathode current collection, and nickel gauze for anode current collection. The anode and cathode chambers were not sealed, allowing the fuel to react with oxidant directly outside the fuel cell. Platinum wires were used as current leads and for cell voltage measurement.

For oxidant flow, oxygen and nitrogen were available. Hydrogen, nitrogen, carbon monoxide, carbon dioxide, methane and hydrogen containing 100 ppm H₂S were available to make the desired fuel gas mixtures. The flows were controlled by mass flow controllers (Bronkhorst, Ruurlo, Netherlands). The fuel could be humidified by either a bubbler operating at 30°C or a steam addition unit (Bronkhorst). The H₂S was introduced in the fuel stream after humidification.

Electrochemical characterisation was performed by measuring the cell voltage as a function of current density (so-called j-V behaviour) and by performing impedance measurements. The j-V characteristics were taken with upgoing current in steps of 1 A, and stabilisation time at each step of 20 seconds, by using a Kikusui electronic load (Kikusui Electronics Corp, Japan) in conjunction with an additional power supply in current-following mode (Delta Elektronika, Zierikzee, Netherlands), which was needed because the electronic load was not able to control the low voltage output of the fuel cell. The impedance spectroscopy measurements were performed at 10 A and 40 A DC load by means of the Gamry FC350 Fuel Cell Monitor (Gamry Instruments, Warminster, USA) in an AC frequency range of 20 kHz to 100 mHz with logarithmic steps and an AC sweep of 1 A. As the membranes were not sealed, it was not possible to perform gas analysis to identify the catalytic activity for methane reforming and the shift reaction. It was however possible to compare the measured open circuit potential with ones calculated from the assumed reactant and product concentrations.

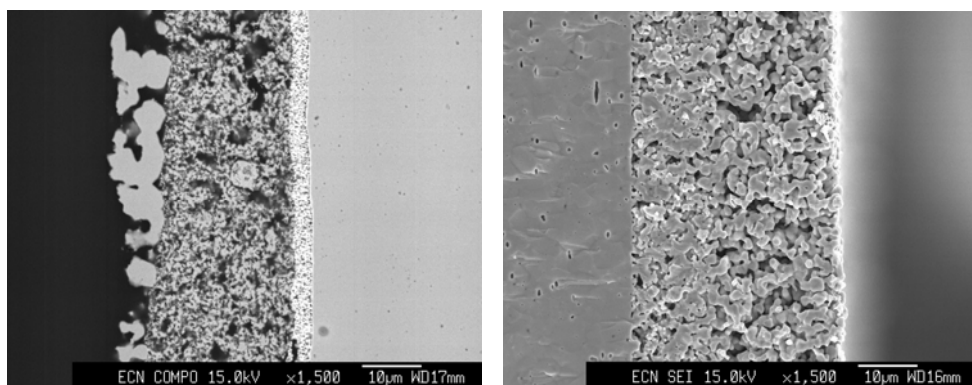


Fig. 1 Micrographs of the used SOFC electrodes (anode left, cathode right)

Results

Table 1 summarizes the fuel compositions which were used to assess the anode activity for the conversion of the main components in biosyngas and the impact of sulfur. By systematically changing the gas composition, insight was obtained in the electrochemical activity for hydrogen and carbon monoxide oxidation, the catalytic activity for methane reforming with either steam or carbon dioxide as well as the impact of H₂S on these reactions. The fuel flows were chosen in such a way that 80% fuel utilization was reached at 40 A in all cases.

Table 1 Fuel compositions used for the anode activity measurements.

Fuel	H ₂ mln/min	CO mln/min	CH ₄ mln/min	CO ₂ mln/min	N ₂ mln/min	H ₂ O mln/min	H ₂ S ppm
1	350	-	-	-	450	34	0-9
2	350	-	-	-	-	15	
3	350	-	-	-	-	147	
4	-	-	87	-	-	147	
5	-	-	87	-	-	294	

6	350	-	-	100	-	20	
7	-	-	87	100	238	18	0-2
8	193	157	-	-	-	147	
9	256	-	23	44	238	44	0-2
10	128	128	23	44	238	44	0-2

Before evaluation under different fuel compositions was started, the membranes were first stabilized at 850°C under 40 A load, fuel consisting of 350 mln/min H₂ and 450 mln/min N₂ humidified at 30°C and oxidant consisting of 400 mln/min O₂ and 1600 mln/min N₂. After switching to a new fuel composition, the membrane was again stabilized under load for 1 hour. Figure 2 to 4 show the j-V curves obtained at 850°C under fuels without sulfur. From these figures it can be seen that H₂, CO and CH₄ are all completely converted. Figure 2 shows that the open circuit voltage (OCV) increases when nitrogen is added to the fuel. As nitrogen is inert under SOFC conditions, it is assumed that the increase is related to improved fuel distribution over the anode surface. Addition of steam to hydrogen causes OCV decrease, and is related to the drop in reactant activity. Addition of CO₂ also causes OCV decrease, which indicates that part of the CO₂ reacts with H₂ to form H₂O by the water-gas shift reaction. Figure 3 shows that H₂ can be replaced with CO without observing any difference in performance, suggesting that CO is as easily oxidized as H₂. It is unknown whether CO is directly oxidized, or that the water-gas shift reaction is involved. From figure 4 it can be seen that methane reforming occurs with both CO₂ and H₂O. The OCV under steam reforming and dry reforming conditions are comparable, suggesting that the methane is reformed with CO₂ or H₂O to the same extent. The impact of sulfur is shown in figure 5, which makes clear that oxidation of hydrogen and carbon monoxide are not affected by sulfur. In contrast to that, the reforming of methane is largely affected when sulfur is added. Addition of 2 ppm H₂S to fuel 7 caused deactivation (not shown), and fuels which only partly consisted of methane showed current limitation at the point where all hydrogen and CO were converted.

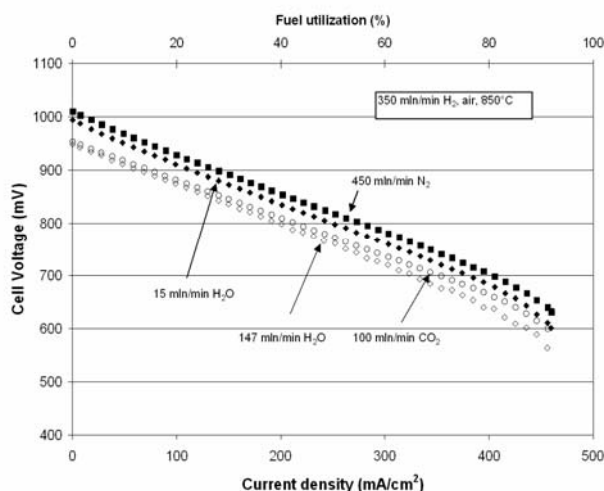


Fig. 2 Impact of N₂, H₂O, and CO₂ addition on the performance under hydrogen

The observed sulfur tolerance under hydrogen is higher than reported in literature for Ni/YSZ anodes [4]. This is probably related to the use of GDC instead of YSZ. Together with Ni, GDC is an active electrocatalyst for hydrogen oxidation [5], with appreciable sulfur tolerance [6]. This benefit of using GDC is much less when methane has to be reformed, as the catalytic activity of GDC for methane reforming has been reported to be much lower than that of nickel [7]. Looking at the integration with a gasifier, it means that when the gasifier is operated in such a way that all methane is converted, relatively high sulfur concentrations are allowed. When, for some reason, methane is still present, the fuel should be cleaned on sulfur before it is efficiently converted with the used Ni/GDC anode.

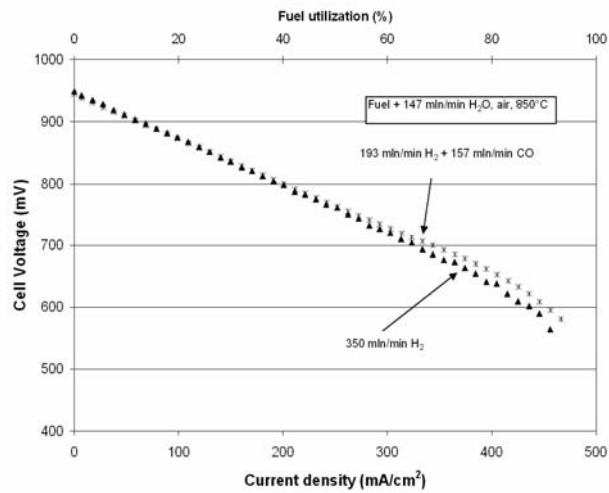


Fig. 3 Performance after partial substitution of hydrogen with CO

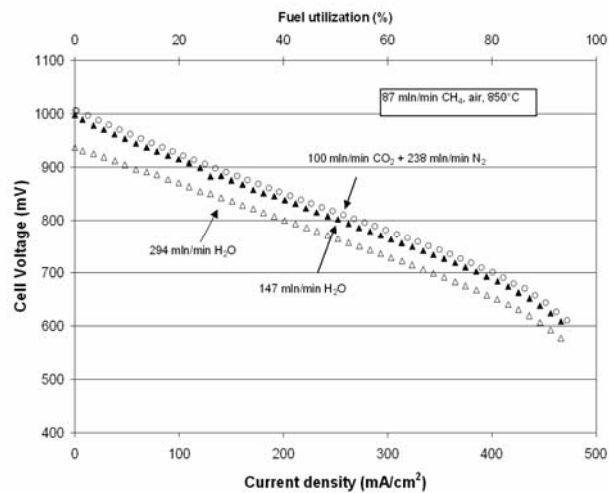


Fig. 4 Impact of CO₂ and H₂O addition on the performance under methane

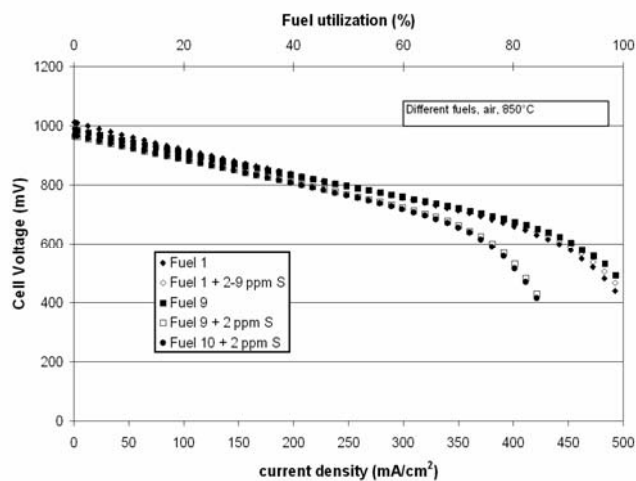


Fig. 5 Impact of sulfur on the performance. The fuel compositions are explained in Table 1.

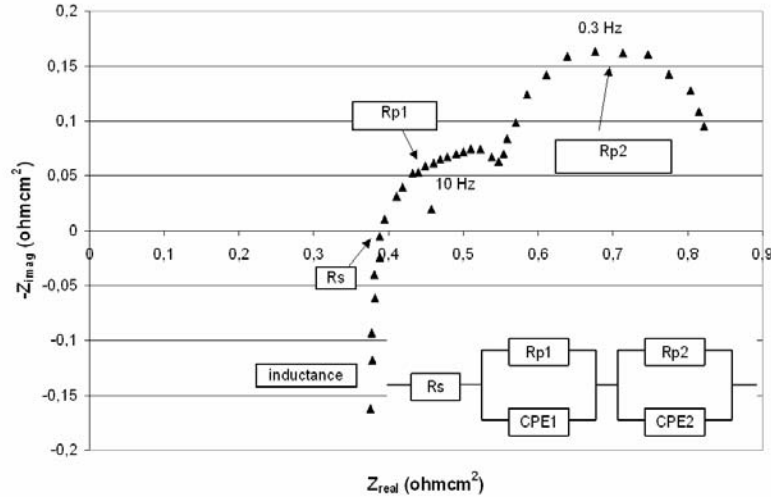


Fig. 6 Typical impedance spectrum (Nyquist plot) obtained at 850°C on a SOFC membrane

A typical example of the obtained impedance spectra is shown in figure 6. The high frequency intercept, which can be seen at around 80 Hz, is further denoted as series resistance R_s . In addition, two polarisation arcs can be seen. The arc with the highest frequency is a depressed semi-circle with a turnover frequency of around 10 Hz and denoted as R_{p1} . The arc with the lowest frequency is a semi-circle with a turnover frequency of 0.3 Hz, from now on denoted as R_{p2} . The impedance spectra were fit with the equivalent circuit shown in figure 6 in the frequency domain of 0.1 to 80 Hz, with the aim to reveal the contributions from the electrolyte and the electrodes. The series resistance R_s , which only depends on temperature, has an average value of 0.32 Ohm cm^2 at 850°C and 0.16 Ohm cm^2 at 920°C , and can be attributed to the electrolyte ionic conductivity [8]. Also R_{p1} depends only on temperature, and amounts 0.24 Ohm cm^2 at 850°C and 0.14 Ohm cm^2 at 920°C . In contrast to R_s and R_{p1} , R_{p2} depends heavily on the gas composition, and increases with temperature. In order to find the origin of R_{p2} , the obtained resistances were plotted against the average (composition at 50% of the applied DC load) and final reactant activity (100% of the applied DC load) in the anode fuel, and assuming that nitrogen is an inactive species. The clearest dependence is found when the final reactant activity is used, figure 7. Another striking observation is that it seems unimportant what chemically active species are involved. This means that perfect mixing of the chemically active species occurs in the direction perpendicular to the membrane surface. The observed dependence of R_{p2} on the reactant activity corresponds with that of the polarisation arc below 1 Hz predicted by Takano et al [9], who ascribed this arc to changes in the electromotive force due to the AC amplitude, and depending on the oxidant and fuel composition, DC load, the retention time of the gases and temperature. It implies that R_{p1} is likely to be a summation of anode and cathode contributions, and that R_{p2} , although it will contribute to the slope of the j-V curve, should be excluded from the determination of the cell resistance as it is not a materials characteristic. On basis of the obtained results, the total cell resistance ($R_s + R_{p1}$) would become 0.6 Ohm cm^2 at 850°C , and 0.3 Ohm cm^2 at 920°C .

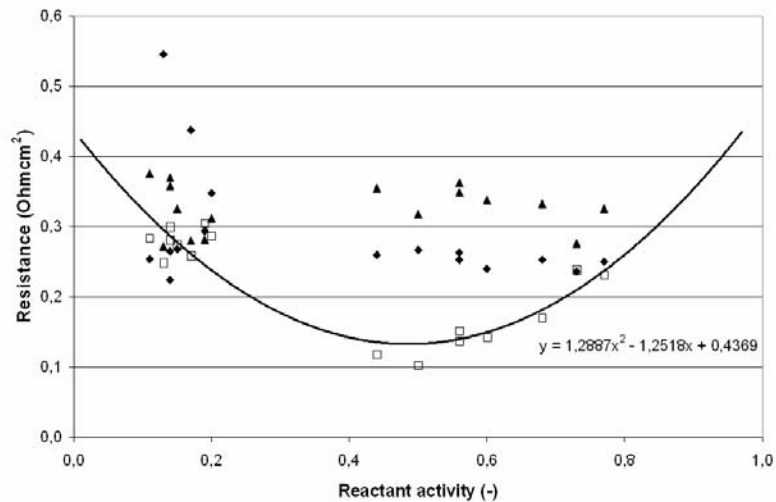


Fig. 7 R_s , R_{p1} , and R_{p2} as a function of reactant activity at 850°C

The SOFC endurance behaviour under biosyngas was tested at 850°C and 920°C under fuel compositions which can be expected from the gasification of wood in air-blown and steam-blown gasifiers after total cleaning on trace components, see figure 8 and 9. After heating to 850°C, the anode was exposed to reducing atmosphere and left at open circuit conditions for 24 hours under fuel consisting of 350 mln/min H_2 and 450 mln/min N_2 humidified at 30°C and 2000 mln/min synthetic air. The cells were then operated at 850 °C and 400 mA/cm² current density, and a slow increase of the cell voltage was observed in time. After switching to biosyngas, the electrochemical performance was initially lower but increased in time to 670 mV, and reached the same level as under hydrogen. After heating to 920°C, the performance stabilized at around 750 mV for both fuels. Finally the membranes were cooled with the anode exposed to H_2/N_2 mixture. Inspection of the anode microstructure made clear that the anode top layer consisting of pure nickel had sintered during operation. The microstructure of the anode functional layer and the oxide layer adjacent to the electrolyte did not change. It makes clear that stable electrochemical performance can be obtained under clean biosyngas. The measured electrical output amounts 2600 W/m² at 850°C, and 3000 W/m² at 920°C.

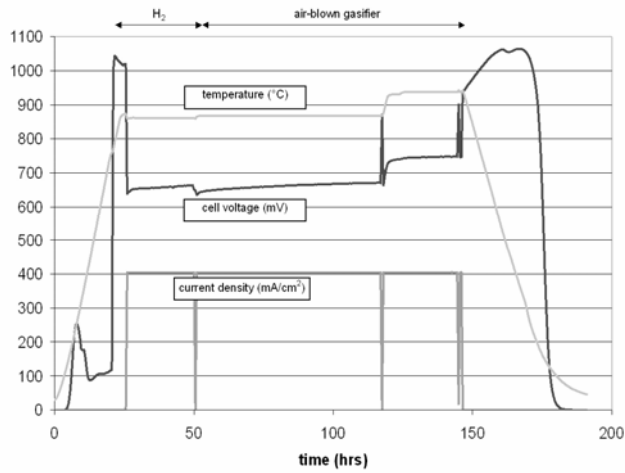


Fig. 8 Electrochemical performance at 850 and 920°C under biosyngas from an air-blown gasifier

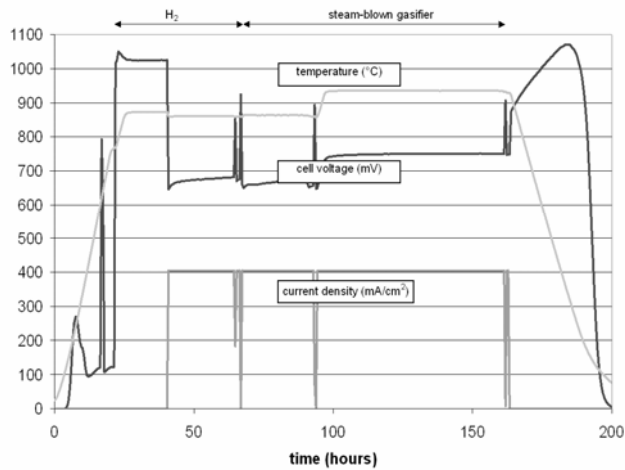


Fig. 9 Electrochemical performance at 850 and 920°C under biosyngas from a steam-blown gasifier

Conclusions

The electrochemical performance of planar, state-of-the-art SOFC membranes from InDEC with Ni/GDC anode have been assessed under clean synthetic biosyngas compositions from air-blown or steam-blown gasifiers. At 80% fuel utilisation, stable electrochemical performance has been obtained, with a power output of 2600 W/m² at 850°C, and 3000 W/m² at 920°C. Sulfur deactivates the Ni/GDC anode for methane reforming, but not for the oxidation of hydrogen and carbon monoxide. AC impedance measurements have revealed that the cell resistance amounts 0.6 Ohmcm² at 850°C and 0.3 Ohmcm² at 920°C.

Acknowledgements

The investigations were supported by the European Commission within the 6th Framework Program (STREP BioCellus, Biomass Fuel Cell Utility System, Contract No: 502759).

References

- [1] Karl J and Karellas S, 2004, "Highly Efficient SOFC Systems with Indirect Gasification", Proceedings of the 6th European Solid Oxide Fuel Cell Forum, 2, pp 534-545
- [2] Aravind PV, Ouweltjes JP, Woudstra N and Rietveld G, 2004, "SOFC Performance with Biomass-Derived Gas", Proceedings of the 6th European Solid Oxide Fuel Cell Forum, 3, pp 1514-1523
- [3] Aravind PV, Ouweltjes JP, Heer E de, Woudstra N and Rietveld G, 2005, "Impact of Biosyngas and its Components on SOFC Anodes", Electrochemical Society Proceedings, 7, pp 1459-1467
- [4] Matsuzaki Y and Yasuda I, 2000, "The Poisoning Effect of Sulfur-Containing Impurity Gas on a SOFC anode: Part I. Dependence on Temperature, Time, and Impurity Concentration", Solid State Ionics, 132, pp 261-269
- [5] Marina OA, Bagger C, Primdahl S and Mogensen M, 1999, "A Solid Oxide Fuel Cell with a Gadolinia-Doped Ceria Anode: Preparation and Performance", Solid State Ionics, 123, pp. 199-208
- [6] Kim H, Vohs JM and Gorte R, 2001, "Direct Oxidation of Sulfur-Containing Fuels in a Solid Oxide Fuel Cell", Chem. Commun., pp 2334-2335
- [7] Ramirez-Cabrera E, Atkinson A and Chadwick D, 2004, "Catalytic Steam Reforming of Methane over Ce_{0.9}Gd_{0.1}O_{2-x}", Applied Catalysis B; Environmental, 47, pp 127-131
- [8] Yamamoto O, Takeda Y, Kanno R, Kamiharai T, 1989, "Electrical Conductivity of Polycrystalline Tetragonal Zirconia", J. of Mat. Sci. Letters, 8, pp 198-200
- [9] Takano K, Nagata S, Nozaki K, Monma A, Kato T, Kaga Y, Negishi A, Inagaki T, Yoshida H, Hosoi K, Hoshino K, Akbay T and Akikusa J, 2004, "Numerical Simulation of a Disk-Type SOFC for Impedance Analysis under Power Generation", J. of Pow. Src., 132, pp 42-51